



# Improved reservoir modeling with time-lapse seismic data integration

John R. Waggoner, WesternGeco

Copyright 2003, SBGf - Sociedade Brasileira de Geofísica.

This paper was prepared for presentation at the 8<sup>th</sup> International Congress of The Brazilian Geophysical Society, held in Rio de Janeiro, Brazil, September 14 -18, 2003.

Contents of this paper were reviewed by The Technical Committee of The 8<sup>th</sup> International Congress of The Brazilian Geophysical Society and do not necessarily represent any position of the SBGf, its officers or members. Electronic reproduction, or storage of any part of this paper for commercial purposes without the written consent of The Brazilian Geophysical Society is prohibited.

## Abstract

Time-lapse 3D, or 4D, seismic studies have generated several good published case studies to date that clearly demonstrate the utility of the 4D seismic information. Many of these papers focus on the geophysics of generating and interpreting the 4D result. This paper extends that body of work by focusing on integrating the 4D result with common reservoir management tools, such as material balance, reservoir simulation, and history matching. After summarizing the integration methods, they are applied to a Gulf of Mexico case study. While history matching results should never be considered unique, they do give some insight into the structure of the reservoir that should be considered for optimal reservoir management, and provide an indication of the impact of 4D information in history matching.

## Introduction

Time-lapse 3D (or 4D) seismic data has proven to be a significant benefit to managing reservoirs<sup>1,2,3</sup> in virtually all cases in which the seismic data has been acquired, processed, analyzed, and interpreted for the purpose of identifying fluid movement within the reservoir. In addition, 4D information has also been shown to be useful when legacy (acquisition not optimized for 4D) seismic data is analyzed, although the best results require that the seismic surveys be reprocessed prior to 4D analysis and interpretation. Either way, the unique character of 4D seismic information, in providing spatially resolved fluid changes within the reservoir, provides an understanding of reservoir architecture and flow that allows the reservoir to be managed more effectively and efficiently.

This paper describes only two elements of the time-lapse seismic workflow employed in the entire project, so as to focus on those issues that integrate the 4D result with reservoir management. The first of these is a material balance calculation that reconciles 4D-interpreted produced fluid volume with the known produced fluid volume. Called Production Analysis 4D, this method serves to check the suitability of 4D processing and generate a filtered 4D result that identifies meaningful time-lapse anomalies.

The other element utilizes reservoir production data along with the seismic data to improve the reservoir model through history matching. This technique allows a quantitative, rather than a visual, interpretation of the time-lapse seismic results. The resulting improvement in the reservoir simulation model provides a direct linkage to reservoir management tools, so that the knowledge gained from the time-lapse study can be better used to manage the reservoir's future performance.

## Production analysis of 4D seismic data

Variations of seismic attributes give a spatial indication of where reservoir changes have occurred. Intuitively, if thickness data are available, a link between volumes of fluid produced (the product of area, thickness, porosity, and saturation change) and seismic attribute variation may be defined. Then, seismic variation above a fixed threshold in a given seismic grid cell corresponds to local variation of reservoir volumes, while below the threshold it represents noise. A volume of produced reservoir fluid, as a function of the threshold, can be computed by adding together cells interconnected with wells. The derived volumetric information can be calibrated using the known volume of fluid produced between the base and monitor times. This procedure<sup>4,5</sup>, termed Production Analysis of 4D data (PA4D), was originally developed for dry gas reservoirs, but has since been extended for gas condensate and black oil reservoir fluids.

## Seismic History Matching

Reservoir flow modeling is a key element of reservoir management, so integrating the 4D information into the reservoir model represents a challenge in any 4D project designed to have a quantitative impact on reservoir management. This challenge was met with the application of a semi-automatic iterative procedure known as Seismic History Matching (SHM)<sup>6</sup>, which can be briefly summarized by the following iterative optimization procedure, starting with an initial reservoir simulation model:

1. Perturb SHM parameter in reservoir model.
2. Simulate fluid flow on reservoir model.
3. Generate synthetic 4D attribute from simulator output.
4. Compute objective function comprising the synthetic/measured 4D mismatch and the simulated/measured production data mismatch.
5. Accept or reject the perturbation applied in step 1, according to optimization method used.
6. Loop to step 1, and continue until a satisfactory stopping criteria is met.

## Application

These 4D reservoir management tools have been applied to Agip's Grand Isle Block 102 asset in the Gulf of Mexico<sup>7</sup>. The reservoir is a retrograde condensate gas reservoir located approximately 110 miles south of New Orleans. The reservoir consists of Pliocenic sand deposited on the marine shelf as a part of a delta complex, with a southwest dipping feature of 21 degrees. The structure is bounded on the northeast, southeast and northwest by faults, without linkage to active aquifers. The fluid originally trapped was a fairly rich retrograde condensate gas, with an approximate oil/gas ratio (OGR) of 100 STB/MMSCF. A first 3D survey was acquired in 1993, production started in May 1994, then a second survey was acquired in July 1996, after  $51 \times 10^9$  SCF of gas and  $3.58 \times 10^6$  STB of gas condensate had been

recovered from the reservoir. During that period, wells' OGRs decreased fairly rapidly, indicating a probable liquid dropout in the reservoir. The acquisitions were not optimized for time-lapse analysis, hence they may be defined as legacy data, but the two surveys have been reprocessed specifically for this 4D project. Figures 1 and 2 show amplitude and acoustic impedance sections for the two surveys.

**PA4D** was applied to the time-lapse impedance maps generated at the G102 horizon to verify the 4D reprocessing and to assess uncertainties in the difference image. Figure 3a shows the map of impedance difference (monitor – base), where the difference is constructed by subtracting relative impedance maps that have been averaged over a 40 ms window below the top reservoir horizon. The blue color indicates decreased impedance and the red indicates increased impedance. Even though the reservoir is located at x values greater than 733000, there are considerable difference anomalies seen throughout the survey area.

The PA4D result is shown in Fig. 3b, zoomed in to show the reservoir unit in more detail. The area shown, in conjunction with the reservoir thickness definition in the reservoir simulation model, represents a volume of produced fluid that is consistent with the observed production data. Therefore, Fig. 3b can be viewed as a 'filtered' version of the map in Fig. 3a, where areas dominated by both random and coherent noise have been largely eliminated. All other anomalies shown in Fig. 3a can be interpreted as noise and not relevant to the production of fluid in the reservoir.

**SHM** is performed in the simulation grid domain, so the implicit fluid change information contained in the 4D attribute map must first be resampled onto the simulation grid, as shown in Fig. 4. Figure 4a is the change in acoustic impedance at the top reservoir horizon in the seismic grid domain, including a box highlighting the subset of the survey covering the simulation grid shown in Fig. 4b. The simulation grid used in this study was the Eclipse model provided at the beginning of the project, consisting of 64 x 37 x 5 cells, with 7595 active cells. White cells on the right of Fig. 4b model represent parts of the model not covered by the 4D attribute shown in Fig. 4a. The resampled result in the simulation domain is considerably smoother than the 4D attribute in the seismic domain as a result of the larger cell dimension in the simulation grid.

Figure 5 shows the measured relative acoustic impedance at the time of the base survey, monitor survey, and difference between the two, all in the simulation grid displays to be used for the remainder of this paper. The primary difference between the display format in Fig. 5 and Fig. 4b is that only active cells are shown, and the simulation grid is indicated by black lines. The well locations are shown by red dots.

The initial porosity model is shown in Fig. 6a, with the corresponding synthetic acoustic impedance variation reported in Fig. 6b, both giving evidence of the measured seismic character shown in Fig. 5a. Note that the synthetic difference image, Fig. 6c, still requires a further calibration to improve the coherence with the measured seismic difference image, Fig. 5c.

SHM was run to 2636 iterations, with the porosity and impedance change results shown in Fig. 7. The porosity map (Fig. 7a, layer 1 shown, but all layers similar) shows an separation between the main reservoir area around the wells and a 'satellite' area to the northwest. The two areas are connected by some means, but the trend is to place a significant, albeit leaky, barrier between them.

It should be noted that much of the spatial information about the reservoir changes was observed by iteration 317. Since many history matching projects operate on limited time constraints, it should not be assumed that thousands of iterations are required as hundreds are probably sufficient to capture critical reservoir characteristics.

Figure 8 shows the objective function history, falling from 92 to 67 over 317 iterations. Although the objective function falls to 46 after 2636 iterations, the progress was increasingly slow and uneventful. SHM progress is seen to proceed as a series of discrete jumps.

As another way to represent SHM progress, Fig. 9 shows a bubble plot illustrating the locations of model perturbations and the associated decrease in objective function. The figure represents each cell center as a dot. Each bubble corresponds to an accepted perturbation, and its center coincides with the center of the perturbation. The size of the bubble is proportional to the decrease of the objective function, and the shading of the bubble corresponds to direction of perturbation. Porosity increases are represented by shaded bubbles, while porosity decreases are represented by white bubbles. Asterisks indicate the three well locations.

The bubble plot indicates the perturbation coverage in this optimization procedure. While not all cells have been perturbed, all areas of the model have been perturbed, indicating that this global optimisation has sampled the solution space well.

The information contained in this bubble plot is a particularly useful summary of the SHM procedure. In this case, it shows that most of the decrease in objective function comes from perturbations to the center left side of the model. It also shows that porosity decreases, indicated by white bubbles, have the most impact in a band crossing the center of the field. This information can then be used to study the model in more detail to understand why perturbations to the model are so important in this location.

### Conventional History Matching

A conventional history matching (CHM) exercise, based on the original Eclipse extended black-oil model, has been run using the production data included in the SHM optimisation. Here "conventional" refers to the use of production data only. It was not intended to be a comprehensive history match using all the field data typically available.

### Production Data Comparison

Both SHM and CHM improve the match to the available production data very well, as indicated by the cumulative oil production and field oil/gas ratio (FOGR) data plotted in Fig. 10. The curves from the SHM model (SHM, iteration 2636) and CHM model (global pore volume

reduction) are much closer to the history data than from the original model. While not shown here, both the SHM and CHM models were run to predict recovery beyond the history match time period. Two different CHM models, using two very different reservoir property assumptions, were able to match production data well, and even predict production well. This illustrates the weakness of history matches without the spatial constraint provided by 4D results.

#### Impact of 4D Information

This case study was driven by the Agip research department as a way of evaluating 4D technologies, and thus did not have a clear reservoir management objective. However, the 4D information illustrates characteristics of the reservoir that have clear impact on reservoir management. Specifically,

1. The SHM process indicates the existence of a partial barrier between the northern and southern ends of the field. In addition, the reservoir structure is likely much more channel-like than represented in the original reservoir model. Both of these observations have implications on well placement and reservoir management.
2. The improved predictability of the SHM-modified reservoir model, as compared with the original model, indicates that it would have been a much better reservoir management tool over the 5 years since the monitor survey.
3. The 4D information provides a positive constraint on the history matching process. History matching without the 4D information was able to match the production data, with good predictability, by perturbing some global model parameters. However, none of these matches is able to create spatial character in the model, as the seismic history match does.
4. The observation of the partial barrier has prompted the Agip Petroleum operating unit to consider drilling a side-track well to better produce that portion of the field.

#### Conclusion

Production analysis 4D and seismic history matching represent the integration of geophysical data and common reservoir engineering tools. These methods, coupled with high quality seismic data acquisition and processing to generate reliable 4D results, provide valuable information to asset teams challenged with managing today's complex and expensive reservoir developments. Integration of disciplines is required to extract maximum value from the data and generate the maximum benefit to the asset team.

#### Acknowledgement

The author acknowledges the many individuals who worked on the Grand Isle 102 project, both at WesternGeco and Agip, and those who helped develop the PA4D and SHM techniques at WesternGeco.

#### Reference

1. Koster, K., Gabriels, P., Hartung, M., Verbeek, J., Deinum, G., and Staples, R.: "Time-Lapse Seismic Surveys in the North Sea and Their Business Impact," *The Leading Edge*, March 2000, **19**, 3, 286-293.
2. Landro, M., Solheim, O.A., Hilde, E., Ekren, B.O., and Stronen, L.K.: "The Gullfaks 4D seismic study," *Petroleum Geoscience*, August 1999, **5**, 213-226.
3. Strønen, L.K., and Digranes, P.: "The Gullfaks Field – 4D Seismic enhances oil recovery and improves the reservoir description," paper X-33, presented at the 62<sup>nd</sup> EAGE conference, Glasgow, 29 May - 2 June, 2000.
4. Huang, X., Will, R., and Waggoner, J.: "Reconciliation of Time-Lapse Seismic Data with Production Data for Reservoir Management: A Gulf of Mexico Reservoir," paper SPE 65155, presented at SPE EUROPEC, Paris, 24 - 25 October 2000.
5. Waggoner, J., Cominelli, A., Seymour, R., and Stradiotti, A.: "Improved Reservoir Modeling with Time-Lapse Seismic in a Gulf of Mexico Gas Condensate Reservoir," *Petroleum Geoscience*, **9**, No. 1, pp. 61-71, Geological Society, London, UK, February 2003.
6. Huang, X., Meister, L., and Workman, R.: "Reservoir Characterization by Integration of Time-Lapse Seismic and Production Data," paper SPE 38695, presented at the 1997 SPE Annual Technical Conference and Exhibition, San Antonio, Texas, 5 - 8 October, 1997.
7. Waggoner, J., Cominelli, A., Seymour, R., and Stradiotti, A.: "Improved Reservoir Modeling with Time-Lapse Seismic in a Gulf of Mexico Gas Condensate Reservoir," paper SPE 77514, presented at the 2002 SPE Annual Technical Conference and Exhibition, San Antonio, Texas, 29 September - 2 October, 2002.

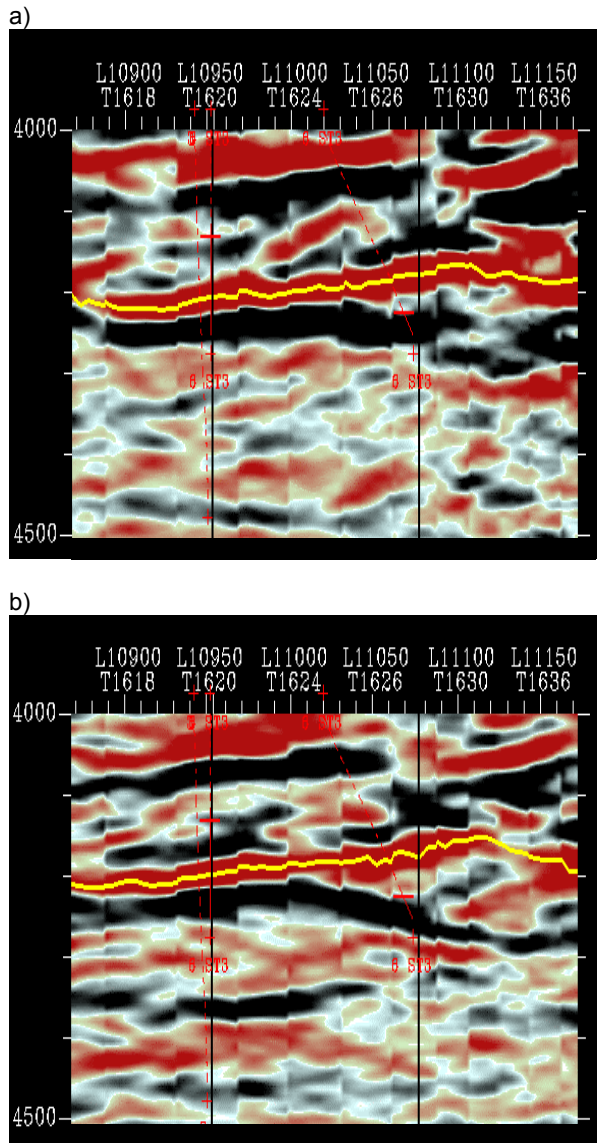


Figure 1: Traverse through amplitude volume for a) base and b) monitor surveys. Traverse path is shown at right. Yellow line indicates the top reservoir horizon interpreted on each survey.

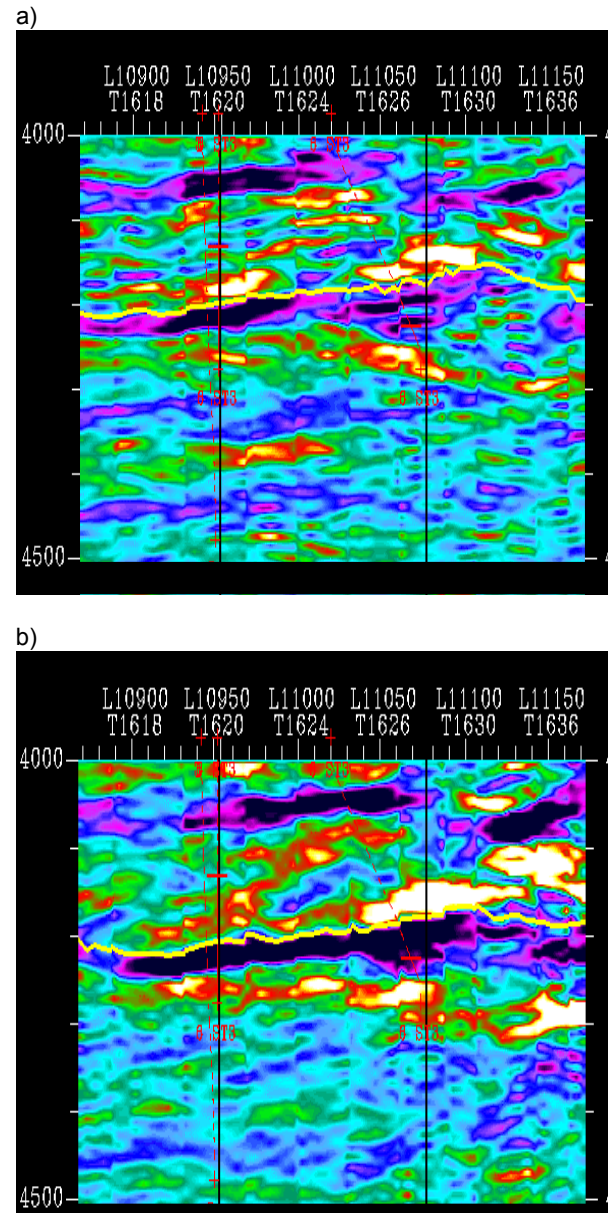
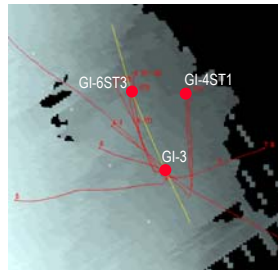


Figure 2: Traverse through acoustic impedance volume for a) base and b) monitor surveys.



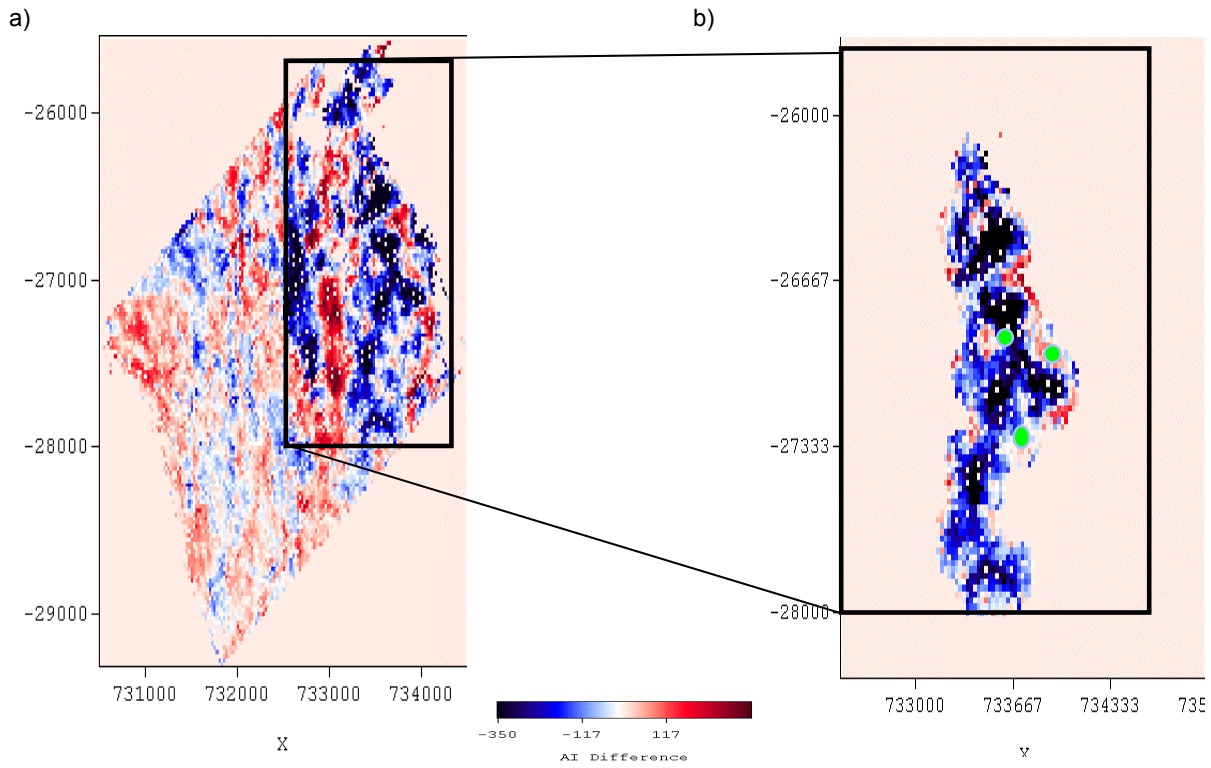


Figure 3: Time-lapse change in acoustic impedance at reservoir horizon a) before application of PA4D, and b) after application of PA4D. The green dots indicate the well locations on the simulation grid.

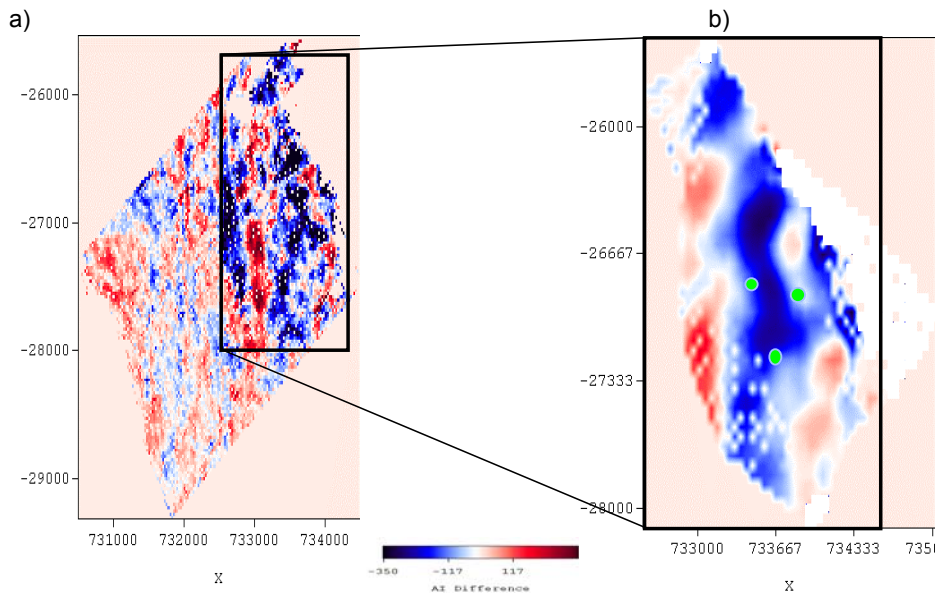


Figure 4: Time-lapse change in acoustic impedance at reservoir horizon, shown on a) the seismic grid and b) after resampling onto the simulation grid. The green dots indicate the well locations on the simulation grid.

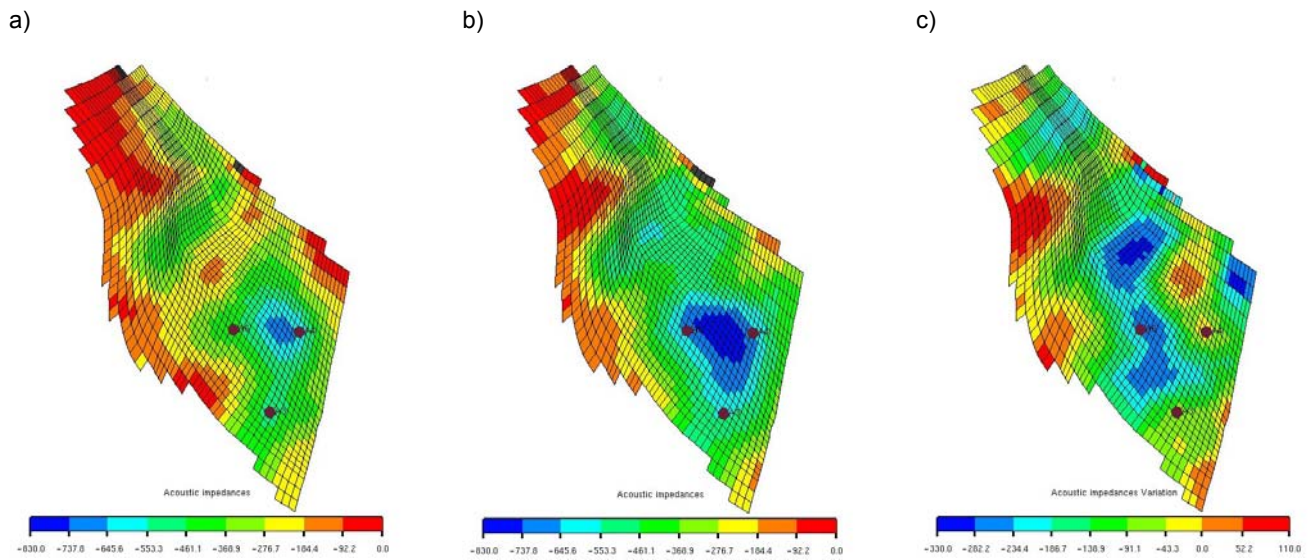


Figure 5: Measured relative acoustic impedance over the reservoir horizon from a) the base and b) monitor surveys, and c) the difference between them. The red dots indicate the well location.

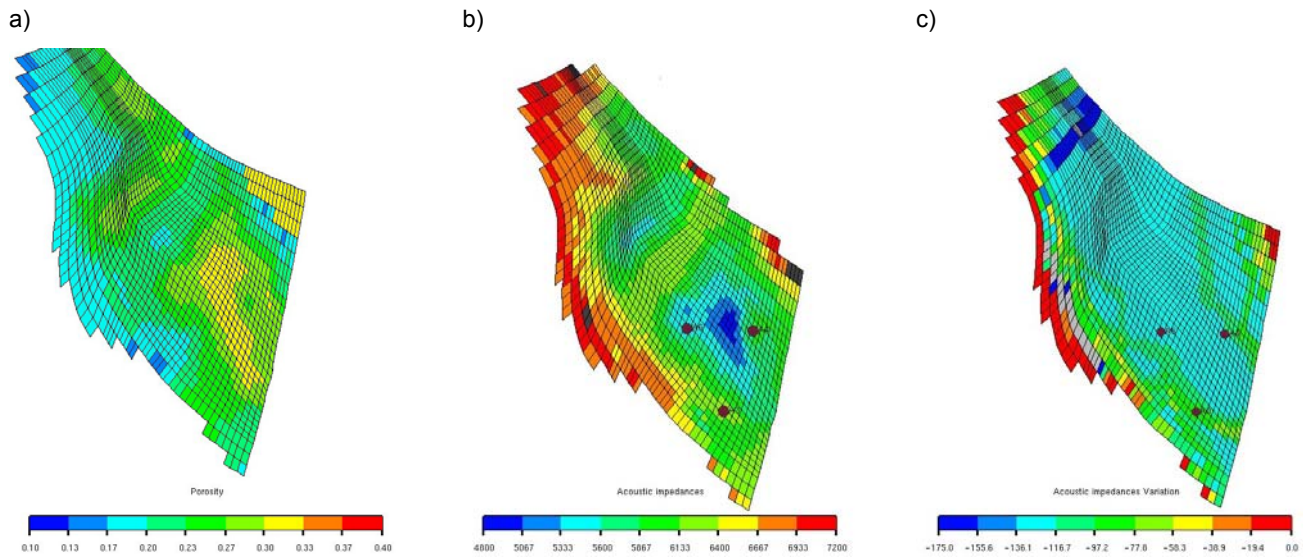


Figure 6 a) Porosity from layer 1 of the new reservoir model, b) associated synthetic acoustic impedance at the time of the base survey, and c) synthetic acoustic impedance change.

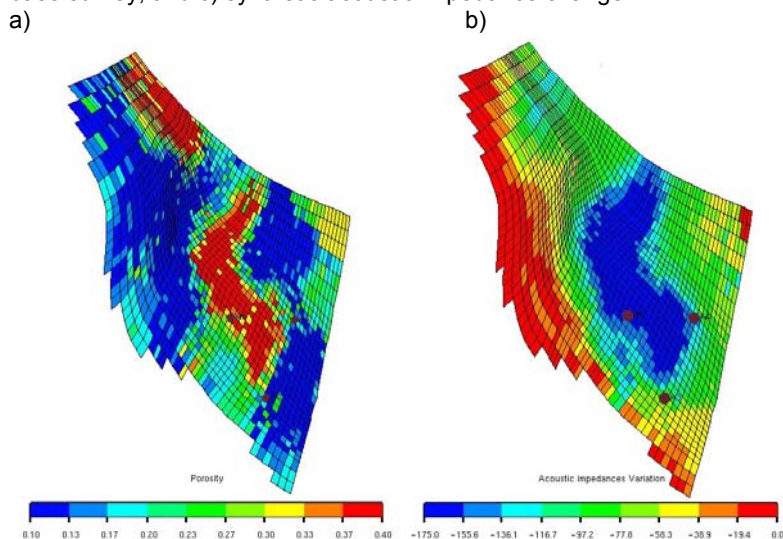


Figure 7: After 2636 iterations, a) porosity from layer 1 of the reservoir model, and b) associated synthetic acoustic impedance change. Compare b) with Fig. 5c.

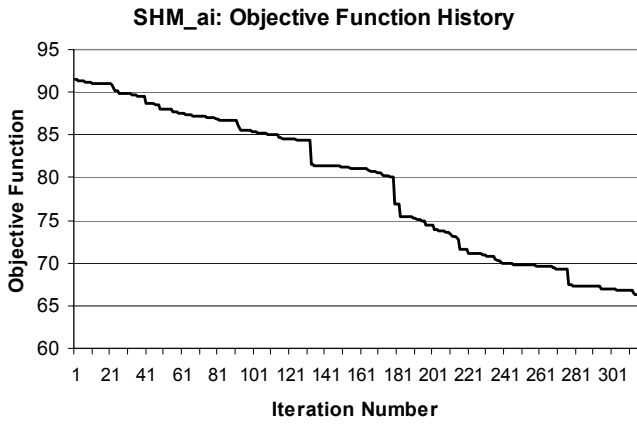


Figure 8: Objective function history up to 317 iterations.

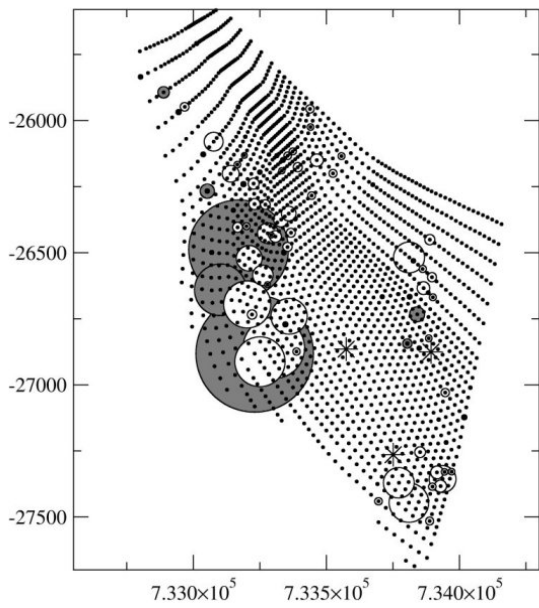


Figure 9: Bubble plot for SHM run, indicating location of perturbations leading to objective function reductions.

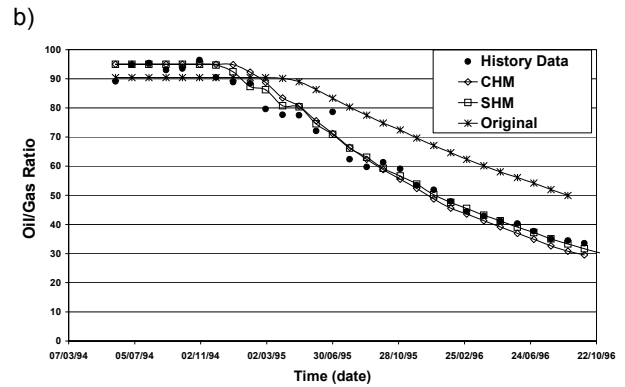
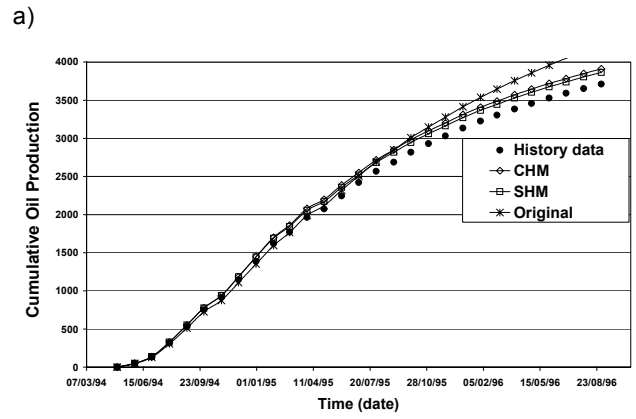


Figure 10: a) Cumulative oil production and b) field oil/gas ratio plots, comparing runs SHM and CHM to the original model and measured history.